Targeting neuroinflammatory pathways using Nanoligomers™ is neuroprotective in prion disease

Sydney J. Risen[1], Sean Boland[1], Sadhana Sharma[3], Grace Weismann[1], Payton Shirley[1], Amelia D. Hines[1], Arielle J. D. Hay[1], Vincenzo Gilberto[1], Stephanie McGrath[2], Anushree Chatterjee[3], Prashant Nagpal[3] and Julie A. Moreno[1]*

Affiliations:

[1]Department of Environmental and Radiological Health Sciences, College of Veterinary Medicine and Biomedical Sciences, Colorado State University, Fort Collins, CO, USA

[2]Clinical Sciences, College of Veterinary Medicine and Biomedical Sciences, Colorado State University, Fort Collins, CO, USA

[3]Sachi Bioworks Inc., Colorado Technology Center, Louisville, CO, USA

Corresponding author:
Julie A. Moreno[1]*
[1]Department of Environmental and Radiological Health Sciences, College of Veterinary Medicine and Biomedical Sciences, Colorado State University; 1680 Campus Delivery. Fort Collins, CO, USA
Email: Julie.Moreno@colostate.edu

Abstract:
Neuroinflammation is a key factor in the development of neurodegenerative diseases, including prion disease. There are currently no effective treatments to halt pathogenesis and progression, which includes accumulation of misfolded proteins, neuroinflammation, and cognitive/behavioral deficits followed by irreversible neuronal death. We hypothesized that downregulation of two key neuroinflammatory targets would be neuroprotective. To test this, we utilized Nanoligomers™ in a prion-diseased mouse to assess the impact on glial inflammation, behavioral/cognition deficits, and loss of neurons. Nanoligomer™ treated mice displayed decreased numbers of glia, and improved behavior and cognitive tests. Critically, the Nanoligomer™ protected the brain from prion-induced spongiotic change, neuronal loss, and significantly increased life span, indicating that Nanoligomer™ inhibition of inflammatory pathways can prevent neuronal death and slow the progression of neurodegenerative diseases.

One-Sentence Summary:

Immunotherapeutic Nanoligomer™ in prion diseased mice opens new treatment avenues for other neurodegenerative diseases.

Neurogenerative diseases are on the rise, impacting millions of people worldwide. These diseases are commonly characterized by glial inflammation and aggregation of misfolded proteins that increase over time, followed by irreversible neuronal loss (*1-3*). Importantly, there are no safe and effective therapies that halt disease progression allowing for neuronal protection. There are many laboratory models commonly utilized for studying these diseases, however few rodent models have all aspects of human neurodegenerative protein-misfolding diseases (NPMDs). Most transgenic mouse models for Alzheimer's disease (AD), AD related diseases, or Parkinson's diseases, display only a few, not all, of the neuronal pathogenesis, behavioral and cognitive deficits, and clinical sign phenotypes. To study therapeutic interventions, we used a wild-type mouse that develops a true NPMD disease following inoculation with prions. Prion diseases are rare neurodegenerative diseases that undergo the common characteristics of NPMDs as the disease progresses. Previous literature has shown therapies developed for prion diseased mice that do not target the misfolded prion protein itself can be translated to other NPMDs (*4, 5*). While a few compounds have been shown to reduce signs of prion disease in mouse models, these compounds have toxic effects in the brain or elsewhere (*4, 6-8*).

Prion diseases result from the native conformation of the cellular prion protein (PrP^{C}) misfolding to the infectious form, PrP^{Sc} (*9, 10*). This misfolding occurs when the alpha helical PrP^{C} protein is conformationally changed to the β-sheet rich PrP^{Sc}, which forms amyloid fibrils and aggregates, causing the disruption of brain homeostasis (*11-13*). Toxic glial inflammation with activation of microglia and astrocytes is an early sign of NPMDs. This is recapitulated in prion disease and is thought to be caused by the aggregation of PrP^{Sc} (*14*). However, it may be that PrP^{Sc} itself is not neurotoxic (*13, 15, 16*), and that disease pathogenesis may result from other cellular stress pathways such as glial inflammation (*17*). Neuroinflammation results in increased oxidative stress, secretion of cytokines, disruption of neural signaling, and glial scarring (*18*) leading to the subsequent damage and loss of synapses, neuronal dysfunction, and neuronal death (*15, 16, 19, 20*). Chronic neuroinflammation is known to be damaging to nervous tissue, and contributes to the development of prion diseases and other NPMDs.

To identify the optimal targets for tackling neuroinflammation cascade, we screened the downregulation of several proinflammatory cytokines (e.g., Interleukin-1β or IL-1β, tumor necrosis factor-alpha or TNF-α, Interleukin 6 or IL-6), inflammasome proteins (e.g., NLRP3, NLRP1), key transcription factors (e.g., nuclear factor kappa-B or NF-κβ), and their combinations (*21*). Non-toxic, targeted, and bioavailable Nanoligomers™ can be administered as naked molecules through injection or inhalation and are designed to cross the blood-brain-barrier (*21-23*). We identified a combination of the NLRP3 inflammasome protein and NF-κβ transcription factor as a viable candidate. During brain stress, similar to NPMDs, there is significant crosstalk between microglia and astrocytes which involves critical inflammatory cell signaling events, such as NF-κB and inflammasome formation. The transcription factor, NF-κB, when translocated into the nucleus causes a number of inflammatory cytokines and chemokines to be transcribed triggering a cascade of microglia and astrocyte inflammation (*24, 25*). Another cell signaling pathway shown to be critical for NPMDs, like prion diseases, is the activation of the inflammasome, specifically initiated by the NLRP3 protein (*26, 27*). We hypothesized that if we can inhibit both of these pathways simultaneously, prion disease progression will slow allowing for neuronal survival, as a proof of principle for other NPMDs. Critically in this study, these Nanoligomers™ were able to save neurons, reduce spongiotic change, decrease behavioral and cognitive deficits, and lower glial inflammation in prion diseased brains once the infection had already been ensued.

Results

Protection of the Nanoligomer™ against prion-induced cognitive and behavioral deficits. Wild-type, C57Bl6/J, (Jackson laboratories) mice were infected intracerebrally with brain homogenates from Rocky Mountain Laboratories (RML) prions or normal brain homogenates (NBH) as the negative control. Nanoligomer™ treatment began at 10 weeks post inoculation (wpi) or approximately 40% of full disease progression and continued until the mice succumbed to prion disease. 10 mg/Kg of the Nanoligomer™ SB_NI_112 or saline as the vehicle, was given either intraperitoneally (i.p.) or intranasally (i.n.) twice a week to both prion and NBH mice (***Fig. 1***). As the diseased progressed and treatment continued,

behavioral assessments including novel object recognition, burrowing, and nesting, were performed at 12 wpi to train and establish a baseline for each experimental cohort (***Fig. 2***). All three behavioral assessments measure hippocampal integrity (*28-30*), the brain region known to show the first clinical pathology including glial inflammation and spongiotic change (*15, 16, 28*).

Mice with prion disease have a significant decrease in the ability to recognize a familiar object, as RML is a prion strain that begins to aggregate within the hippocampus, the brain region essential for memory and learning (*4, 15*). Both i.p. and i.n. SB_NI_112 treatment protected a prion induced deficit in novel object recognition when compared to vehicle treated diseased mice at 22 wpi (***Fig.2B***). The ratio of time the mouse spent with the novel object to the familiar object, seen 24 hours beforehand, was calculated and noted as the discrimination index. The closer the discrimination index is to one, the more intact the hippocampal memory. Both i.p. treated mice ($p<0.0005$, mean discrimination index score: 0.449) and i.n. treated mice ($p < 0.005$, mean discrimination index score: 0.434) had a significant increase in novel object recognition when compared to vehicle (discrimination index of -0.174, ie. preferring the familiar object). At 20 wpi a significant increase in the recognition of the novel object was seen between prion infected mice treated with vehicle and SB_NI_112 i.p. (***Fig. 2A***).

Two other behavioral assessments were performed on the cohorts of mice to compare prion induced deficits with and without SB_NI_112 treatment. Mice were given napkins to nest overnight and scored between one (no nest formed) and five (fluffy nest) starting at 16 wpi. Monitoring of nest formation was found to be significantly higher among i.p. treated mice at 20 wpi ($p > 0.005$), 21 wpi ($p > 0.005$), and 22 wpi ($p > 0.05$) (***Fig. 2C***) compared to vehicle treated. Another hippocampal assay, burrowing, was also monitored. Individual mice were placed in a cage containing a plastic tube filled with food pellets for 30 min to burrow freely. Following the burrowing period, food pellets left in the tubes were weighed and percent burrowed calculated (*29*). Prion diseased mice are known to stop burrowing as disease progresses. Treatment with SB_NI_112 at 20-22 wpi (***Fig. 2D***) showed a trend of protection against burrowing deficits with at p value = 0.09 for the 20 wpi time point (detailed quantitative assessment scoring provided in Methods). The weights of the mice with and without treatment with SB_NI_112 were not significantly different throughout the disease progression, indicating no acute toxicity due to the Nanoliogmer ***(Fig. S1).***

Nanoligomer™ SB_NI_112 treatment reduces glial inflammation. In addition to the behavioral assessments, the potential therapeutic effect on glial pathology was assessed. Brain tissues were collected at 20 wpi. Formalin fixed tissues were processed and embedded into paraffin wax. Once sliced on the microtome, brains were stained for both microglial and astrocytic inflammation (***Fig. 3***). Astrocytic inflammation was identified as S100β+ cells (***Fig. 3A***) and Iba1+ cells denote inflamed microglia (***Fig. 3F***). Four brain regions were assessed: hippocampus, cortex, thalamus and cerebellum. In the thalamic region, both astrocytic and microglial inflammation was significantly suppressed with SB_NI_112 Nanoligomer™ treatment (***Fig. 3C*** and ***Fig. 3H***, respectively) at 20 wpi. Additionally, at the same time point both i.n. and i.p. SB_NI_112 treatment provided significant protection from microglia inflammation in the hippocampus (***Fig.3G***), cortex (***Fig. 3I***), and the cerebellum (***Fig. 3J***).

Neuronal protection using Nanoligomer™ SB_NI_112. A morphologic spongiotic change, or formation of vacuoles, within the brain tissue is a hallmark of prion disease that increases as the disease progresses (*16*). To assess and quantify this change, we used pathologic scoring of the hippocampus, thalamus, cortex, and cerebellum following H&E staining. This revealed protection against spongiotic change in both i.p. and i.n. SB_NI_112 Nanoligomer™ treatment of prion diseased mice (***Fig. 4A and B***) when compared to vehicle treated prion diseased mice. The loss of neurons within the hippocampus following RML prion infection is well established (*4, 15*), therefore we assessed this within our treatment group. Critically, neuronal numbers within the CA1 region of the hippocampus were significantly protected by SB_NI_112 Nanoligomer™ i.p. and i.n. treatment compared to vehicle treated ($p>0.05$, ***Fig. 4D, E***).

Importantly, we see no change in the PK resistant prion protein PrP^{Sc} with Nanoligomer™ treatment (***Fig. 4C***). Therefore, the neuroprotection is independent of the misfolding and aggregation of PrP^{Sc} itself and could be a good avenue of therapy for other NPMDs with differing toxic misfolded proteins.

Clinical scores and survival improved in mice treated with Nanoligomer™. At 22 wpi, vehicle treated mice begin to show a significant increase clinical signs of prion disease (***Fig. 4F***). From 22 wpi to 24 wpi i.p. and i.n. SB_NI_112 treated diseased mice have significantly ($p<0.0001$ and $p<0.0005$ respectively) lower clinical scores than vehicle treated diseased mice. Prion clinical signs included tail rigidity, hyperactivity, ataxia, extensor reflex, tremors, righting reflex, kyphosis, and poor grooming (Movie S1-S5) (*4, 15*). Each sign was rated on a scale from 0-5. All clinical sign scores were combined for a total score. Mice were considered terminal and euthanized after reaching a total score of 9 or above. Date of mice succumbing to prion disease was documented for survival analysis (***Fig. 4G***). Importantly, the lifespan of prion disease mice was significantly increased with i.p. SB_NI_112 Nanoligomer™ treatment ($p>0.05$) compared to vehicle treated mice.

Discussion

The slowing of the progression of neurodegenerative protein misfolding diseases (NPMDs) has proven to be difficult. Many promising treatments are toxic or must be delivered directly to the brain, making translation to human patients challenging. Here, we have successfully used a non-toxic, systemically delivered Nanoligomer™ that protects against prion disease induced neuronal toxicity and death. Protection of cognition/behavioral deficits and the clinical progression of disease is accomplished with the Nanoligomer™ (***Fig. 2***). This Nanoligomer™ specifically inhibits two known inflammatory events, NF-κB and NLRP3 expression, in the brain and significantly decreases microglial and astrocytic inflammation, slowing disease progression (***Fig. 3***). Through the inhibition of glial inflammation neurons were protected, indicated by a decrease in spongiotic change and neuronal loss, independent of a decrease in the misfolded protein itself (***Fig. 4***). Findings show the Nanoligomers™ can slow both early cognitive/behavioral phenotypic changes, subsequent clinical signs, and most importantly neuronal death. Critically, we have identified a treatment for a neurodegenerative disease that can be delivered to the periphery with no toxic effects. These findings of neuroprotection within a prion diseased mouse can be easily translated to other neurodegenerative diseases, as neuroinflammation is a generic pathology irrespective of the misfolded protein.

Materials and Methods.

All materials and methods can be found in Supplement document.

1. H. S. Kwon, S. H. Koh, Neuroinflammation in neurodegenerative disorders: the roles of microglia and astrocytes. *Transl Neurodegener* **9**, 42 (2020).
2. F. Leng, P. Edison, Neuroinflammation and microglial activation in Alzheimer disease: where do we go from here? *Nat Rev Neurol* **17**, 157-172 (2021).
3. M. T. Heneka *et al.*, Neuroinflammation in Alzheimer's disease. *Lancet Neurol* **14**, 388-405 (2015).
4. J. A. Moreno *et al.*, Oral treatment targeting the unfolded protein response prevents neurodegeneration and clinical disease in prion-infected mice. *Sci Transl Med* **5**, 206ra138 (2013).
5. H. J. Kim *et al.*, Therapeutic modulation of eIF2alpha phosphorylation rescues TDP-43 toxicity in amyotrophic lateral sclerosis disease models. *Nat Genet* **46**, 152-160 (2014).
6. K. Nazor Friberg *et al.*, Intracerebral Infusion of Antisense Oligonucleotides Into Prion-infected Mice. *Mol Ther Nucleic Acids* **1**, e9 (2012).
7. J. Bian, H. E. Kang, G. C. Telling, Quinacrine promotes replication and conformational mutation of chronic wasting disease prions. *Proc Natl Acad Sci U S A* **111**, 6028-6033 (2014).
8. R. R. Reimann *et al.*, Differential Toxicity of Antibodies to the Prion Protein. *PLoS Pathog* **12**, e1005401 (2016).
9. S. B. Prusiner, Prions. *Proc Natl Acad Sci U S A* **95**, 13363-13383 (1998).
10. S. B. Prusiner, Novel proteinaceous infectious particles cause scrapie. *Science* **216**, 136-144 (1982).
11. D. C. Gajdusek, Transmissible and non-transmissible amyloidoses: autocatalytic post-translational conversion of host precursor proteins to beta-pleated sheet configurations. *J Neuroimmunol* **20**, 95-110 (1988).
12. J. H. Come, P. E. Fraser, P. T. Lansbury, Jr., A kinetic model for amyloid formation in the prion diseases: importance of seeding. *Proc Natl Acad Sci U S A* **90**, 5959-5963 (1993).
13. J. Collinge, A. R. Clarke, A general model of prion strains and their pathogenicity. *Science* **318**, 930-936 (2007).
14. C. Cunningham *et al.*, Systemic inflammation induces acute behavioral and cognitive changes and accelerates neurodegenerative disease. *Biol Psychiatry* **65**, 304-312 (2009).
15. J. A. Moreno *et al.*, Sustained translational repression by eIF2alpha-P mediates prion neurodegeneration. *Nature* **485**, 507-511 (2012).
16. M. K. Sandberg *et al.*, Prion neuropathology follows the accumulation of alternate prion protein isoforms after infective titre has peaked. *Nat Commun* **5**, 4347 (2014).
17. B. Li, M. Chen, C. Zhu, Neuroinflammation in Prion Disease. *Int J Mol Sci* **22**, (2021).
18. H. Muhleisen, J. Gehrmann, R. Meyermann, Reactive microglia in Creutzfeldt-Jakob disease. *Neuropathol Appl Neurobiol* **21**, 505-517 (1995).
19. G. R. Mallucci, Prion neurodegeneration: starts and stops at the synapse. *Prion* **3**, 195-201 (2009).
20. A. K. K. Lakkaraju *et al.*, Glial activation in prion diseases is selectively triggered by neuronal PrP(Sc). *Brain Pathol*, e13056 (2022).
21. S. Sharma *et al.*, Identifying Optimal Neuroinflammation Treatment Using Nanoligomer™ Discovery Engine. *bioRxiv*, (2022).

22. C. R. McCollum *et al.*, Nanoligomers Targeting Human miRNA for the Treatment of Severe COVID-19 Are Safe and Nontoxic in Mice. *ACS Biomater Sci Eng* **8**, 3087-3106 (2022).
23. S. Sharma, C. Fallgreen, M. M. Weil, A. Chatterjee, P. Nagpal, Screening Immunotherapy Targets to Counter Radiation-Induced Neuroinflammation. *bioRxiv* (2022).
24. B. S. Thawkar, G. Kaur, Inhibitors of NF-kappaB and P2X7/NLRP3/Caspase 1 pathway in microglia: Novel therapeutic opportunities in neuroinflammation induced early-stage Alzheimer's disease. *J Neuroimmunol* **326**, 62-74 (2019).
25. S. A. Liddelow *et al.*, Neurotoxic reactive astrocytes are induced by activated microglia. *Nature* **541**, 481-487 (2017).
26. H. Bai, Q. Zhang, Activation of NLRP3 Inflammasome and Onset of Alzheimer's Disease. *Front Immunol* **12**, 701282 (2021).
27. K. L. Hanslik, T. K. Ulland, The Role of Microglia and the Nlrp3 Inflammasome in Alzheimer's Disease. *Front Neurol* **11**, 570711 (2020).
28. C. Cunningham *et al.*, Synaptic changes characterize early behavioural signs in the ME7 model of murine prion disease. *Eur J Neurosci* **17**, 2147-2155 (2003).
29. R. M. Deacon, J. M. Raley, V. H. Perry, J. N. Rawlins, Burrowing into prion disease. *Neuroreport* **12**, 2053-2057 (2001).
30. G. R. Mallucci *et al.*, Targeting cellular prion protein reverses early cognitive deficits and neurophysiological dysfunction in prion-infected mice. *Neuron* **53**, 325-335 (2007).

Acknowledgments: The authors thank Lab Animal Resources at Colorado State University for their animal husbandry throughout the study.

Funding:
Financial support from National Aeronautics and Space Administration SBIR Contracts 80NSSC21C0242 and 80NSSC22CA116

Author contributions:

Conceptualization: JAM, PN, AC, SM

Methodology: SJR, SB, SS, GW, PS, AH, AJDH, VG

Funding acquisition: SJE, MJM, JLS, EH

Supervision: JAM, PN, AC

Writing –SJR, JAM, PN, AC, SM

Competing interests:

S.S., A.C., and P.N. are employed by the for-profit company Sachi Bioworks where the Nanoligomer technology was developed. A.C. and P.N. are the founders of Sachi Bioworks, and P.N. has filed a patent on this technology.

All other authors have no competing interests.

Data and materials availability: All data are available in the main text or the supplementary materials.

Supplementary Materials:

Materials and Methods
Supplementary Text
Fig. S1: Nanoligomer™ SB_NI_112 does not cause weight loss with twice a week treatment for 14 weeks
Captions for Movies S1 to S5: Nanoligomer™ SB_NI_112 protects prion mice from development of clinical signs at 24 wpi

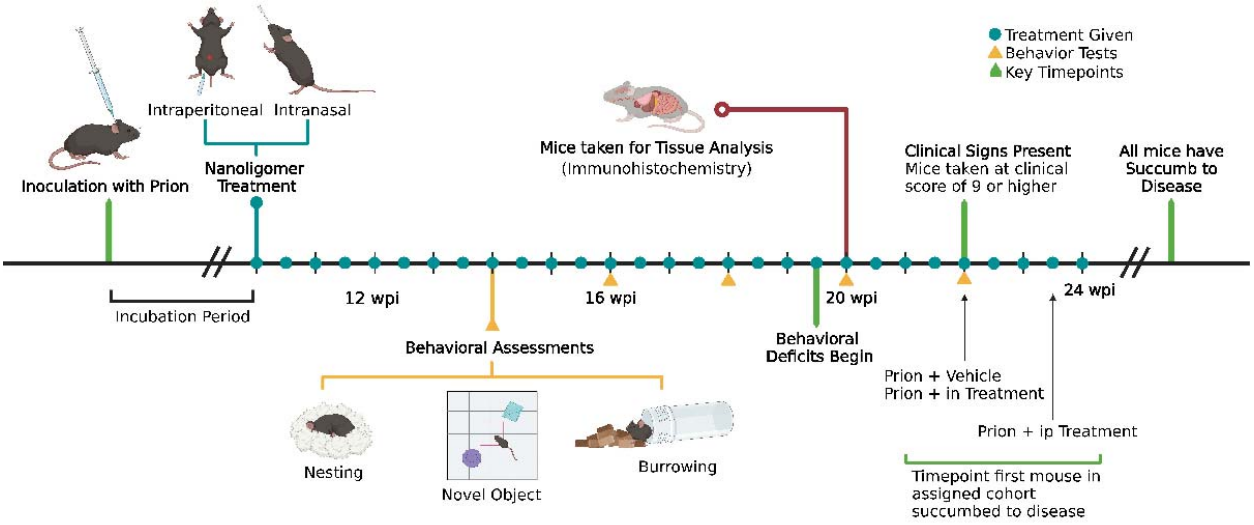

Figure 1. Schematic of Study. Prion diseased mice were treated with Nanoligomers™ or vehicle through intraperitoneal or intranasal routes of exposure, twice a week starting at 10 weeks post inoculation (wpi). Throughout the progression of the disease cognitive, hippocampal specific behaviors and clinical signs were monitored. At 20 wpi brain tissue was dissected for analysis of disease progression including neuroinflammation, spongiotic change and neuronal loss. Graphic created with BioRender.com

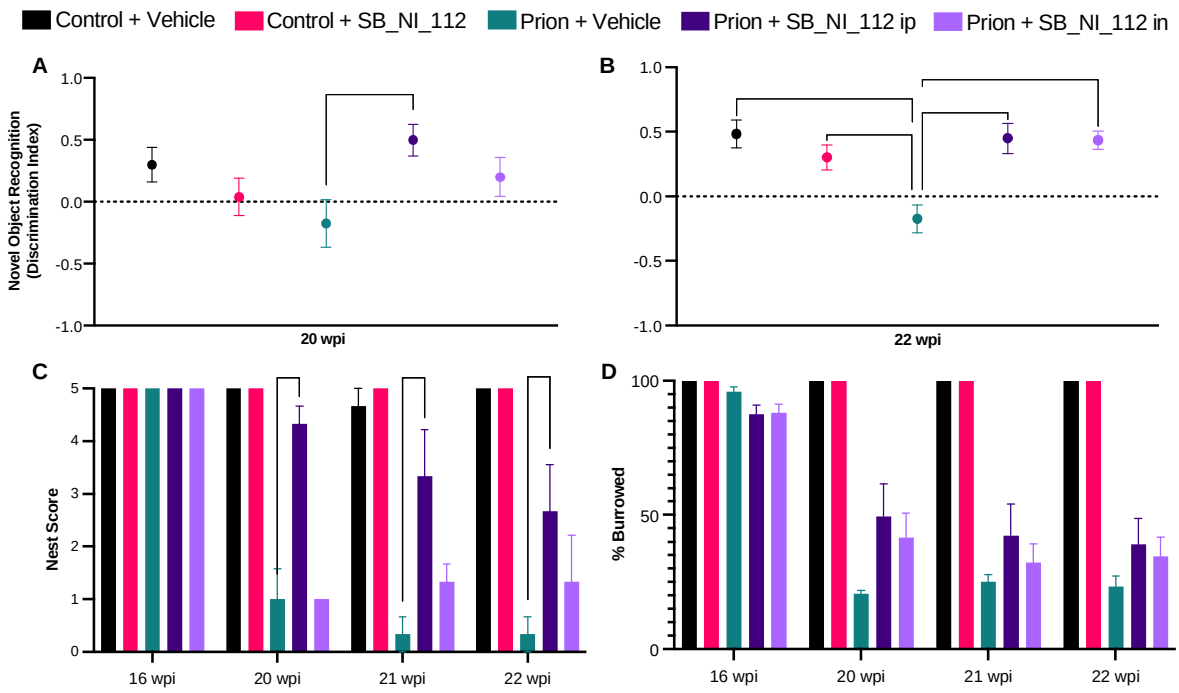

Figure 2. Cognition and behavioral deficits are protected by Nanoligomers™ treated by intraperitoneal route. Mice were monitored for changes in cognition and behavior throughout the disease progression. Nanoligomer™ treatment (SB_NI_112) protected the prion induced deficit in spatial novel object recognition seen in the vehicle treated prion diseased mice following (**A**) intraperitoneal (i.p.) treatments for 20 wpi and (**B**) i.p and intranasal (i.n) at 24 wpi. (**C**) A significant increase in the ability of the mice to build proper nests at 20 and 21 wpi with i.p. treatment of the Nanoligomers™ compared to vehicle treatments was seen. (**D**) No significant change was seen in the hippocampal assay burrowing when mice were treated with the Nanoligomers™ compared to vehicle. N=9 for prion positive i.p. and i.n. groups, N=12 for all other groups. One-way ANOVA and post-hoc Tukey test, error bars = SEM, * $p < 0.05$, ** $p < 0.01$, *** $p < 0.001$, **** $p < 0.0001$, ns = not significant.

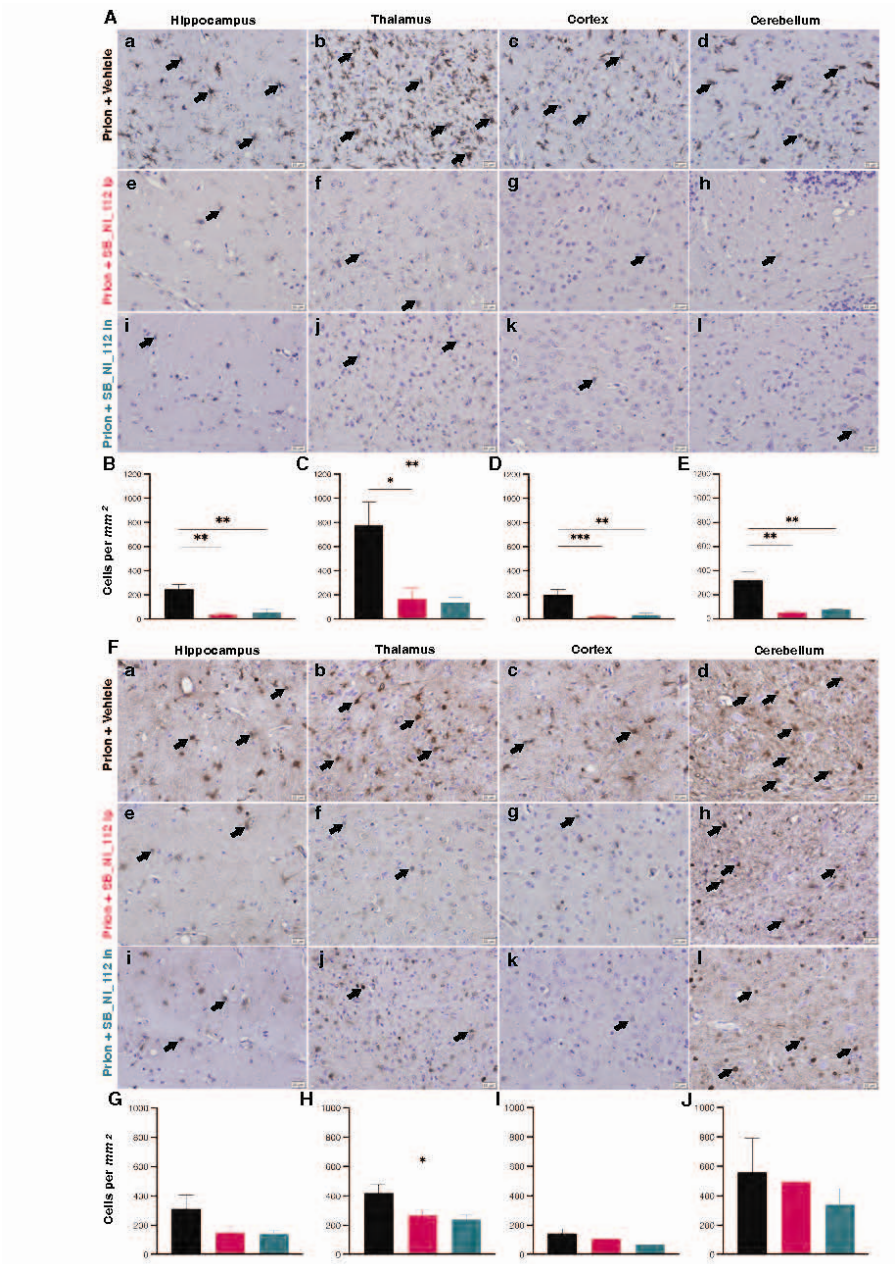

Figure 3. Microglia and astrocytic inflammation are significantly reduced using Nanoligomers in prion diseased mice. (**A**) Representative images of the hippocampus (i, v, ix), thalamus (ii, vi, x), cortex (iii, vii, xi) and cerebellum (iv, viii, xii) brain regions of S100β+ cells, a maker of inflamed astrocytes, with SB_NI_112 intraperitoneal (i.p.) and intranasal (i.n.) treatment. Quantitative analysis of each brain region identifies a significant change in the (**C**) thalamus and a trend of a decrease of inflamed astrocytes in the (**B**) hippocampus and **(D**) cortex and (**E**) cerebellum with treatment. (**F**) Representative images of the hippocampus (i, v, ix), thalamus (ii, vi, x), cortex (iii, vii, xi) and cerebellum (iv, viii, xii) brain regions for IBA1+ cells, a maker for microglia, with and without treatment. Quantitative analysis of each brain region identifies a significant change in the (**G**) hippocampus, (**H**) thalamus, (**I**) cortex and (**J**) cerebellum with both i.n. and i.p. treatment. Arrows represent examples of positive cells. Scale bar = 20μm N=3-4. One-way ANOVA and post-hoc Tukey test *p > 0.05, **p> 0.001, ***p > 0.0001

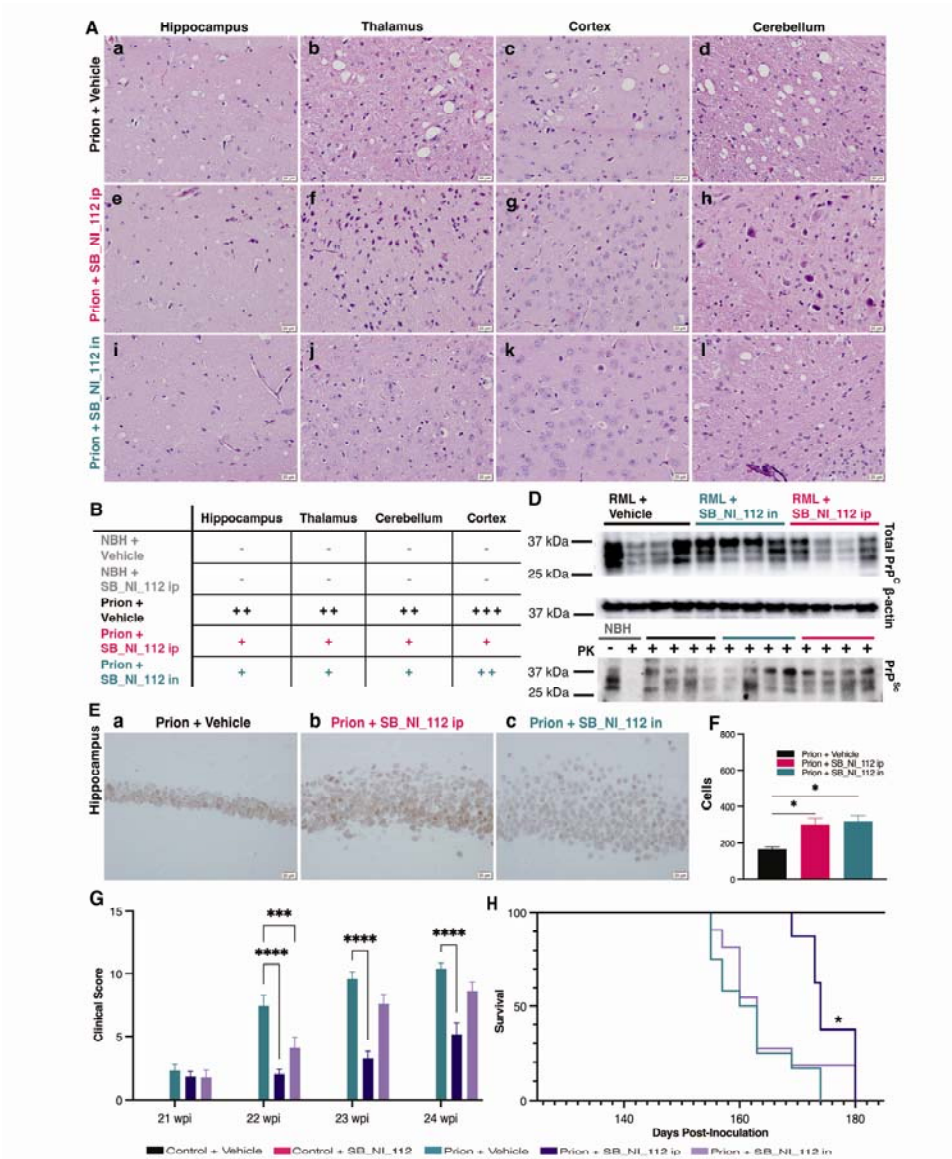

Figure 4. Nanoligomer™ SB_NI_112 is neuroprotective in prion-induced disease model. (**A**) Representative images of the spongiotic change in hippocampus (i, v, ix), thalamus (ii, vi, x), cortex (iii, vii, xi) and cerebellum (iv, viii, xii) brain regions were protected with SB_NI_112 intraperitoneal (i.p.) and intranasal (i.n.) treatment. (**B**) Pathological scoring of each brain region identifies a protection or decrease of pathological score at all brain regions with Nanoligomer™ treatment. Arrows point to spongiotic change. **(C)** Cellular prion protein (PrP^{C}) and misfolded neurotoxic protein PrP^{Sc} show no significant change between treatment groups (**D**) Representative images of the NeuN + cells (neuronal cell bodies) in the CA1 region of the hippocampus. (**E**) Significant decrease in the number of neurons lost at 20wpi with treatment via i.p. and i.n. SB_NI_112. Scale bar = 20µm N=3-4. (**F**) Prion clinical scores were monitored and shown to be protected by both i.n. and i.p. treatment at 22 wpi and continued to protective with i.p. until 25 wpi. (**G**) The life-span of these prion diseased mice was significantly elongated with i.p.

nanoligomer treatment. N=9 for prion positive i.p. and i.n. groups, N=12 for all other groups. One-way ANOVA and post-hoc Tukey test, error bars = SEM, *p > 0.05 *** p< 0.001, **** p< 0.0001

Supplementary Materials for

Targeting neuroinflammatory pathways using Nanoligomers™ is neuroprotective in prion disease

Sydney J. Risen[1], Sean Boland[1], Sadhana Sharma[3], Grace Weismann[1], Payton Shirley[1], Celine Campos[1], Amelia Hines[1], Vincenzo Gilberto[1], Arielle D. Hay[1], Stephanie McGrath[2], Anushree Chatterjee[3], Prashant Nagpal[3] and Julie A. Moreno[1]*

Correspondence to: Julie.Moreno@colostate.edu

This PDF file includes:

Materials and Methods
Supplementary Text

Fig. S1
Captions for Movies S1 to S5

Other Supplementary Materials for this manuscript include the following:

Movies S1 to S5

Materials and Methods

Ethics Approval

Mice were euthanized by deeply anaesthetizing with isoflurane followed by decapitation. All mice were bred and maintained at Lab Animal Resources, accredited by the Association for Assessment and Accreditation of Lab Animal Care International, in accordance with protocols approved by the Institutional Animal Care and Use Committee at Colorado State University.

Nanoligomer™ development

Nanoligomers™ were synthesized using previously published procedure (*1-5*). Briefly, the Sachi bioinformatics platform was used to identify the lead Nanoligomer™ sequence of the DNA/RNA binding domain. The desired peptide molecules were synthesized using solid phase peptide synthesis, and conjugated to the gold nanoparticle, for high-throughput purification and delivery. The concentration of the peptide molecules and Nanoligomers™ was quantified using ultraviolet-visible optical spectroscopy.

Mice and Brain homogenates

C57Bl/6 (Jackson Labs) mice were inoculated intracranially with 30µl of 1% Rocky Mountain Laboratories (RML) mouse-adapted scrapie, or normal brain homogenate (NBH). Mice were monitored for weight loss and euthanized after showing signs of terminal prion disease. 20% brain homogenates were made in phosphate-buffered saline using beads and a tissue homogenizer (Benchmark Bead Blaster 24) and stored at -80C.

Nanoligomer™ Administration. At 10 weeks post RML prion or NBH inoculation, mice were treated two times per week either intraperitoneally (i.p.) or intranasally (i.n.) with 10mg/kg of Nanoligomer™ SB_NI_112 diluted in sterile saline. Mice receiving treatment intranasally were anesthetized prior to administration and laid in an intranasal apparatus that controlled isoflurane throughout the intranasal procedure.

Cognitive assay: Novel Object Recognition

Mice were tested in a rectangular arena (28cm x 43cm). Mice were habituated to the arena seven days before testing. On day one of habituation, mice were permitted to explore the empty arena for ten minutes. On day two of habituation, two identical objects (constructed with Legos) were placed in the arena, approximately 10 cm from the walls with 20 cm distance between. Each mouse was placed in the arena for ten minutes of exploration. During day one of testing, mice were placed in the arena with two identical objects and were given 5 minutes of exploration. On day two of testing, one of the known objects was replaced by a novel object, and the 5-minute exploration was filmed using a 1080P FHD Mini Video Camera. All objects and the arena were cleansed thoroughly between trials to ensure the absence of olfactory cues. Time exploring both the known and novel object was calculated blinded. Discrimination index calculated following Absolute vs Relative Analysis protocol (*6*).

Hippocampal Behavioral assays: Burrowing and Nesting

Briefly, mice were placed in a cage with a PVC tube full of food pellets, as described (*7*). The natural tendency of rodents is to displace (burrow) the food pellets. The percentage of burrowing activity is calculated from the difference in the weight of pellets in the tube before and after 30 minutes. To test nesting, three fresh napkins were placed in each cage. After 24 hours, cages were examined for nesting activity. Nests were scored on a scale of 0-5, where 0 represents no nesting activity, and 5 represents a high-quality nest that provides shelter for the mice.

Clinical Scoring of mice

Eight key clinical signs were monitored in mice daily beginning at 20 wpi. Clinical signs included tail rigidity, hyperactivity, ataxia, extensor reflex, tremors, righting reflex, kyphosis, and poor grooming. Each sign was rated on a scale from 0-5. All clinical sign scores were combined for a total score. Mice considered terminal and euthanized after reaching a total score of 9 or above.

Immunohistochemistry

Paraffin-embedded brains were sectioned at 5 µm and stained with NeuN antibody (1:250; Cell Signaling) for CA1 neuronal counts. Astrogliosis was detected with S100β antibody (1:400; Abcam). Iba1 antibody (Abcam; 1:400) was used for microglial counts. Nonspecific binding was blocked before primary antibodies with 10% Horse Serum

(Vector Labs). A biotinylated secondary antibody (Vector Labs) was used, and stain was visualized with diaminobenzidine reagent. All images were taken with CellSens? software and counted with CellSens (Iba1 and S100β) or manually (NeuN).

Immunoblotting

Brain homogenates were isolated using phosphate buffered saline (PBS) supplemented with Phos-STOP and Complete protease inhibitors (Roche). A BCA Protein Assay kit (Thermo Scientific) was used to quantify protein concentration of lysates, and 25 µg of protein was digested with 20 µg/mL proteinase K (PK) (Roche) for PrP^{Sc} blots for 1 hour at 37C. Digestion was terminated with 2mM PMSF. For PrP^{C} blots, 10 µg of samples was used. Samples were run using 4-20% acrylamide SDS page gels (BioRad) and then transferred onto PVDF blotting paper (MilliPore). Primary antibody Bar-224 (Cayman Chemical) was used at 1:5,000 in 5% non-fat milk in tris buffered saline with tween and HRP-conjugated secondary antibodies at 1:5,000 (Vector Laboratories). The protein antibody complex was visualized using SuperSignal West Pico PLUS Chemiluminescent Substrate (Thermo Scientific) and visualized with the BioRad ChemiDoc MP.

Supplementary Text

Clinical signs and weights

Previous work shows that Nanoligomers™ have no toxicity when given intraperitoneally to mice over a period of 24 hours (*1-4*). To monitor acute toxicity of Nanoligomers™ in mice treated for 15 weeks, weights and overall health of the mice were monitored in all five groups: 1.) Normal brain homogenate (NBH) + vehicle, 2.) NBH + i.p. Nanoligomer™ SB_NI_112, 3.) Prion + vehicle, 4.) Prion + vehicle, 5.) Prion + i.p. Nanoligomer™ SB_NI_112 and 5.) Prion + i.n. Nanoligomer™ SB_NI_112. It has been well established that prion diseased mice show a significant decrease in weight as the disease progresses seen here as well (*8-12*), however this is not amplified with Nanoligomer™ SB_NI_112, indicating no acute toxicity (***Fig. S1***).

Unlike most laboratory mouse models of neurodegeneration, prion diseased mice actually have the disease and early and late clinical signs are well characterized (*8-12*). These clinical signs can be assessed throughout the disease progression. Here we show clasping of hind limbs (***Movie S1***), righting reflex (***Movie S2***) and weakness of hindlimbs (***Movie S3***) in prion + vehicle mice but not in the Prion + i.p. Nanoligomer™ SB_NI_112 treated.

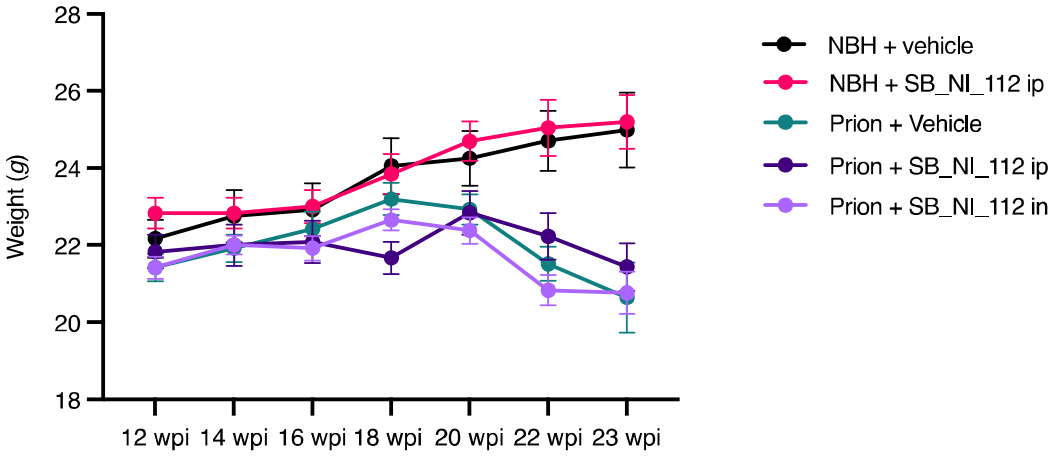

Fig. S1. No change in weights due to the Nanoligomer treatment. Prion diseased mice with vehicle, i.p. and i.n. SB_NI_112 treatment all significantly decrease in weight as the disease progresses, but this does not occur in normal brain homogenate (NBH) mice vehicle or SB_NI_112 i.p. N = 9-12 per group.

Movie S1-S3.

Movies S1 to S3: The Nanoligomer™ SB_NI_112 prevents prion diseased induced clinical signs. Each video shows aged matched normal brain homogenate (NBH) (left video), prion-infected mice treated with vehicle (middle video) or with Nanoligomer™ SB_NI_112 (right video) at 24 weeks post infection (wpi). The vehicle prion diseased mice show early clinical signs of prion disease such as hind limb clasping (***Movie S1***) and later confirmatory signs of prion disease include an impaired righting reflex (***Movie S2***) and dragging of hind limbs (***Movie S3***) due to weakness and paralysis. Yet, mice are protected from developing clinical signs with twice a week i.p. treatment of the Nanoligomer™ SB_NI_112.

References

1. S. Sharma *et al.*, Identifying Optimal Neuroinflammation Treatment Using Nanoligomer™ Discovery Engine. *bioRxiv*, (2022).
2. C. R. McCollum *et al.*, Nanoligomers Targeting Human miRNA for the Treatment of Severe COVID-19 Are Safe and Nontoxic in Mice. *ACS Biomater Sci Eng* **8**, 3087-3106 (2022).
3. C. M. C. Colleen R. McCollum, Nolan J. O'Connor, Thomas R. Aunins, Tristan X. Jordan, Keegan Rogers, Stephen Brindley, Jared M. Brown, Prashant Nagpal, Anushree Chatterjee, Safety and biodistribution of Nanoligomers™ targeting SARS-CoV-2 genome for treatment of COVID-19. *bioRxiv* **500688**, (2022).
4. S. Sharma, C. Fallgreen, M. M. Weil, A. Chatterjee, P. Nagpal, Screening Immunotherapy Targets to Counter Radiation-Induced Neuroinflammation. *bioRxiv* (2022).
5. S. S. Colleen M. Courtney, Christina Fallgren, Michael M. Weil, Anushree Chatterjee, Prashant Nagpal, Reversing radiation-induced immunosuppression using a new therapeutic modality,. *Life Sciences in Space Research*, (2022).
6. L. M. Lueptow, Novel Object Recognition Test for the Investigation of Learning and Memory in Mice. *J Vis Exp*, (2017).
7. G. R. Mallucci *et al.*, Targeting cellular prion protein reverses early cognitive deficits and neurophysiological dysfunction in prion-infected mice. *Neuron* **53**, 325-335 (2007).
8. J. A. Moreno *et al.*, Oral treatment targeting the unfolded protein response prevents neurodegeneration and clinical disease in prion-infected mice. *Sci Transl Med* **5**, 206ra138 (2013).
9. M. Halliday *et al.*, Partial restoration of protein synthesis rates by the small molecule ISRIB prevents neurodegeneration without pancreatic toxicity. *Cell Death Dis* **6**, e1672 (2015).
10. D. Peretti *et al.*, RBM3 mediates structural plasticity and protective effects of cooling in neurodegeneration. *Nature* **518**, 236-239 (2015).
11. H. Radford, J. A. Moreno, N. Verity, M. Halliday, G. R. Mallucci, PERK inhibition prevents tau-mediated neurodegeneration in a mouse model of frontotemporal dementia. *Acta Neuropathol* **130**, 633-642 (2015).
12. J. A. Moreno *et al.*, Sustained translational repression by eIF2alpha-P mediates prion neurodegeneration. *Nature* **485**, 507-511 (2012).